Thermodynamic assessment of the oxidative steam reforming of biomass fast pyrolysis volatiles

Gartzen Lopez[a,b], Irati Garcia,[a] Aitor Arregi[a], Laura Santamaria[a], Maider Amutio[a], Maite Artetxe[a], Javier Bilbao[a], Martin Olazar[a]

[a]Department of Chemical Engineering, University of the Basque Country UPV/EHU, P.O. Box 644 - E48080 Bilbao (Spain). gartzen.lopez@ehu.es

[b]IKERBASQUE, Basque Foundation for Science, Bilbao, Spain

Abstract

The joint process of pyrolysis-steam reforming is a novel and promising strategy for hydrogen production from biomass; however, it is conditioned by the endothermicity of the reforming reaction and the fast catalyst deactivation. Oxygen addition may potentially overcome these limitations. A thermodynamic equilibrium approach using Gibbs free energy minimization method has been assumed for the evaluation of suitable conditions for the oxidative steam reforming (OSR) of biomass fast pyrolysis volatiles. The simulation has been carried out contemplating a wide range of reforming operating conditions, i.e., temperature (500 to 800 ºC), steam/biomass (S/B) ratio (0 to 4) and equivalence ratio (ER) (0 to 0.2). It is to note that the simulation results under steam reforming (SR) conditions are consistent with those obtained by experiments. Temperatures between 600 and 700 ºC, S/B ratios in the 2-3 range and ER values of around 0.12 are the optimum conditions for the OSR under autothermal reforming (ATR) conditions, as they allow attaining high hydrogen yields (10 wt.% by mass unit of the biomass in the feed), which are only 12 to 15 % lower than those obtained under SR conditions.

Keywords; Hydrogen; biomass; oxidative reforming; thermodynamic study; Gibbs; simulation; pyrolysis; oxygenates reforming

1. Introduction

The environmental concern associated with global warming is boosting the replacement of fossil fuels by alternative renewable and clean energy sources. Within this scenario, hydrogen is expected to have a key role in the way towards energy sustainability. However, the current hydrogen production is mainly based on the reforming of fossil fuels, such as natural gas, oil streams and coal [1-3]. Thus, processes aimed at hydrogen production from alternative and sustainable sources, such as thermochemical processes for the valorization of biomass and waste, are gaining increasing attention. Amongst them, gasification [4-6], pyrolysis [7,8] and steam reforming (SR) of biomass derived products (bio-oil) [3,9,10] have proven to be viable for the production of syngas and hydrogen. However, these processes face important challenges for their full scale implantation, such as the excessive tar formation in the gasification process, which hinders syngas potential applications in synthesis processes and energy production [11,12]. Steam reforming main limitations are associated with the fast deactivation of the catalyst and reaction endothermicity [3,10,13,14]. Furthermore, biomass pyrolysis faces the endothermicity of the process and, especially, the limited quality of the bio-oil (low heating value, poor stability and corrosiveness), which hinder its direct use as fuel [15,16].

In order to overcome these challenges associated with the reforming of bio-oil, oxidative steam reforming (OSR) has been proposed [17]. In fact, co-feeding oxygen not only allows reaching a neutral energy balance in the reforming process, but also promotes the attenuation of catalyst deactivation, as has been reported in the processing

of different feeds [18-20]. Thus, OSR can delay coke formation by favoring the combustion of carbon deposits, thereby improving the stability of the catalyst compared to SR conditions [21]. Besides, the energy requirement of the reforming reaction is solved, since partial oxidation of pyrolysis volatiles is promoted when the reforming is carried out in an oxidative regime [17]. However, oxygen addition must be carefully controlled to avoid significant reductions in hydrogen production and other operational problems, such as metallic catalyst oxidation and the subsequent loss of activity [22].

This study deals with the potential of oxidative steam reforming for the treatment of biomass fast pyrolysis volatiles for hydrogen production, based on the simulation of thermodynamic equilibrium results. Gibbs free energy minimization method is proposed for the simulation of reactor performance under different operating conditions in order to determine hydrogen yields and reaction enthalpies, and establish autothermal conditions in the OSR of biomass fast pyrolysis volatiles. The simulation of equilibrium conditions has been previously applied for the prediction of the OSR of different feedstocks, such as hydrocarbons [23], oxygenates [17,24,25] and bio-oil [17,26].

The aim of the current study is to progress in the development of an original pyrolysis and in-line reforming technology by adopting the OSR strategy. This process has proven to have a great potential for hydrogen production from biomass under SR conditions, as it allows obtaining yields of around 10 wt. % when the process is fine-tuned [27-35]. The authors have developed a combination of a conical spouted bed reactor (CSBR) for the pyrolysis step and a fluidized bed reactor (FBR) for the reforming one to perform pyrolysis-reforming in continuous regime. A scheme of this process is shown in Figure 1.

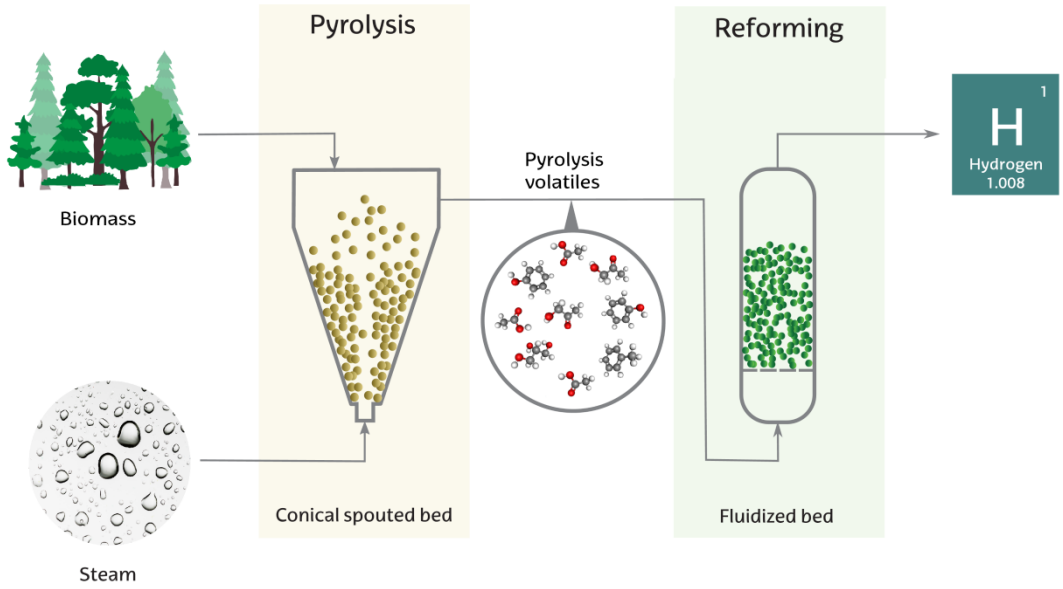

Figure 1. Dual reactor (CSBR-FBR) for the fast pyrolysis and SR or OSR of in-line volatiles.

This dual reactor system has proven to perform well in the valorization of different biomasses, plastics and their mixtures [27,32,36-38]. The use of a CSBR ensures operation under fast pyrolysis conditions with an efficient conversion of biomass into bio-oil [39,40], as well as a great flexibility for treating different biomasses and solid wastes and for process scaling up [41-43]. In addition, the mixing regime and high heat and mass transfer rates characteristic of FBRs lead, on the one hand, to lower carbonaceous material deposition than fixed beds [44,45] and, on the other hand, to isothermicity in the OSR process, avoiding hot spots in the catalyst bed.

This strategy has several advantages in comparison with the pyrolysis process with an in-situ reforming catalyst. The integration of both reactors in the same unit allows selecting the suitable reaction system for each process, as well as the optimum conditions in the pyrolysis and in-line reforming steps [46]. Thus, the production of oxygenates in the biomass pyrolysis (first step) and H_2 in the reforming process (second

89 step) are maximized under optimum operating conditions. Besides, catalyst efficiency is
90 improved, since it treats the whole stream of volatiles formed in the pyrolysis reactor,
91 and a lower deactivation rate is observed, since the direct contact of the reforming
92 catalyst with the biomass and its impurities is avoided [5,47].

93 In order to perform a reliable simulation of the OSR process, this study considers a real
94 composition of the volatile stream obtained in previous biomass fast pyrolysis studies in
95 a CSB [48]. Moreover, the results obtained under SR conditions in previous studies [27]
96 were used for the validation of the proposed calculation approach.

97 **2. Methodology**

98 2.1. Simulation of the reforming of biomass pyrolysis volatile stream

99 The reforming of biomass fast pyrolysis volatiles was simulated following a
100 thermodynamic analysis using the Gibbs free energy minimization method. This
101 approach is especially interesting in complex systems with multiple compounds and
102 reactions, as is the case of biomass derived product reforming, given that it does not
103 require equilibrium constants to determine equilibrium compositions. Pro II 10.1
104 software was used for simulation, and the equation of state the one by Soave-Redlich-
105 Kwong. The reactor has been considered isothermal and the reaction performed at
106 constant pressure.

107 The model used is shown in Figure 2 and includes the reforming reactor inlet streams,
108 i.e., oxygenates, gaseous products (CO, CO_2, H_2, hydrocarbons), steam, and oxygen, as
109 well as a mixer and the Gibbs free reactor. The basis considered in the simulation was
110 100 kg h^{-1} of biomass (with a moisture of 10 wt.%) fed into the pyrolysis-reforming
111 process. The streams of pure oxygen and steam were fixed according to the equivalence
112 ratio (ER) and steam/biomass (S/B) ratio, respectively. The S/B ratio was defined based

on the steam and biomass feed rates injected into the pyrolysis step; however, the ER was defined based on the volatiles fed into the reforming process.

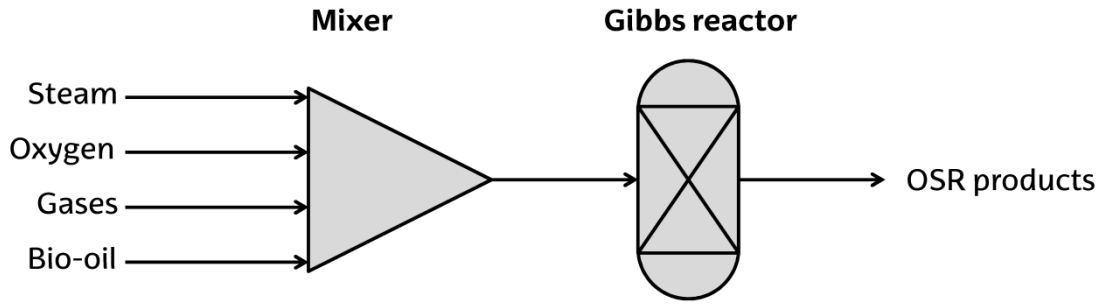

Figure 2. Scheme of the calculation model used in the thermodynamic study.

The following main reactions were considered in the evaluation of the results obtained in the reforming simulation:

Methane steam reforming: $CH_4 + H_2O \Leftrightarrow CO + 3H_2$ (1)

Oxygenates reforming: $Oxygenates + H_2O \rightarrow CO + H_2$ (2)

Water gas shift (WGS): $CO + H_2O \Leftrightarrow CO_2 + H_2$ (3)

Methane dry reforming: $CH_4 + CO_2 \Leftrightarrow 2CO + 2H_2$ (4)

Oxygenates dry reforming: $Oxygenates + CO_2 \rightarrow CO + H_2$ (5)

Hydrogen oxidation: $H_2 + ½O_2 \Leftrightarrow H_2O$ (6)

Methane oxidation: $CH_4 + 2O_2 \rightarrow CO_2 + 2H_2O$ (7)

Oxygenates oxidation: $Oxygenates + O_2 \rightarrow CO_2 + H_2O$ (8)

The composition of the streams at the inlet of the reforming reactor was established based on the results obtained in a previous pyrolysis study carried out by continuously feeding biomass (pine wood sawdust) into a conical spouted bed reactor (CSBR) at 500

130 ºC [48]. It is to note that this composition is extremely complex, with more than 110
131 oxygenate compounds identified, which were grouped into chemical families (phenols,
132 saccharides, ketones, acids and so on). In order to determine accurately the real
133 composition of these oxygenates, the most representative compounds of these families
134 were considered in the simulator database, for which their molecular weight and
135 elemental composition were also taken into account. The composition of the oxygenate
136 stream (condensable bio-oil fraction) used in the simulation is shown in Table 1. The
137 composition of the remaining volatiles (non-condensable gaseous products) is
138 summarized in Table 2. As overserved, this stream is simpler than that of oxygenates
139 and was taken from previous results [48]. Based on their composition, the average
140 molecular formula of the pyrolysis volatile stream to be reformed is $CH_{1.23}O_{0.44}$,
141 excluding water.

142 **Table 1.** Composition of the oxygenate stream used for the simulation of the
143 reforming step.

Compound	**Formula**	**Concentration (wt. %)**
Aldehydes		**3.86**
Formaldehyde	CH_2O	0.46
Acetaldehyde	C_2H_4O	0.21
Acrolein	C_3H_4O	0.15
Glutaraldehyde	$C_5H_8O_2$	0.57
Heptanal	$C_7H_{14}O$	0.07
Salicylaldehyde	$C_7H_6O_2$	0.42
Vanillin	$C_8H_8O_3$	1.97
Alcohols		**2.66**
Methanol	CH_4O	0.91
Glycerin	$C_3H_8O_3$	1.47
1-Phenyl-1-propanol	$C_9H_{12}O$	0.27
Acids		**3.62**

Formic acid	CH_2O_2	0.23
Acetic acid	$C_2H_4O_2$	1.47
Propanoic acid	$C_3H_6O_2$	0.19
Acetic anhydride	$C_4H_6O_3$	1.20
Benzoic acid	$C_7H_6O_2$	0.54
Phenols		**20.60**
Phenol	C_6H_6O	0.53
2-Methyl phenol	C_7H_8O	0.51
3-Methyl phenol	C_7H_8O	0.38
1.2-Benzenediol	$C_6H_6O_2$	5.41
1,4-Benzenediol	$C_6H_6O_2$	0.35
4-Ethyl phenol	$C_8H_{10}O$	0.42
2-Methoxy-phenol	$C_7H_8O_2$	5.66
p-Isopropenyl phenol	$C_9H_{10}O$	0.46
Styrene glycol	$C_8H_{10}O_2$	1.51
Benzyl acetate	$C_9H_{10}O_2$	1.42
Ethyl phenyl acetate	$C_{10}H_{12}O_2$	3.95
Furans		**4.41**
Furan	C_4H_4O	0.94
Furfural	$C_5H_4O_2$	0.11
2-Furanmethanol	$C_5H_6O_2$	0.99
Tetrahydro-2-furanmethanol	$C_5H_{10}O_2$	2.36
Saccharides		**5.92**
Dilactide	$C_6H_8O_4$	2.07
Dilactic acid	$C_6H_{10}O_5$	3.85
Ketones		**8.53**
Acetone	C_3H_6O	0.89
1-Hydroxy-2-propanone	$C_3H_6O_2$	2.04
Methyl propyl ketone	$C_5H_{10}O$	0.36
Cyclohexanone	$C_6H_{10}O$	3.44
Levulinic acid	$C_5H_8O_3$	0.36
Acetovanillone	$C_9H_{10}O_3$	1.45
Unidentified		**16.74**
1.3-Benzenediol	$C_6H_6O_2$	16.74

Water	H_2O	**33.67**

Table 2. Gas product composition used for the simulation of the reforming step.

Compound	Formula	Concentration (wt. %)
Carbon dioxide	CO_2	44.66
Carbon monoxide	CO	46.12
Hydrogen	H_2	0.05
Methane	CH_4	4.90
Ethylene	C_2H_4	1.17
Ethane	C_2H_6	0.79
Propylene	C_3H_6	1.01
Propane	C_3H_8	0.63
2-Butene	C_4H_8	0.66

The simulation of the reforming step was carried out in a wide range of operating conditions: temperature, 500-800 ºC; S/B ratio, 0-5 (corresponding to S/C molar ratios from 0 to 9.6, by mass unit of the volatiles fed into the reforming step), and ER, 0-0.2.

2.2. Experimental runs

The experiments for the validation of the results obtained in the thermodynamic study were carried out in a unit that combines a conical spouted bed reactor (CSBR) and a fluidized bed reactor (FBR) for the pyrolysis and catalytic steam reforming steps, respectively. The dimensions and other details of the pyrolysis-reforming plant, such as those concerning gas and solid feeding systems, condensation device and gas cleaning equipment, were described in detail in previous papers [27,37]. The biomass used in the experiments was pine wood sawdust with a particle size between 1 and 2 mm, with a moisture content of 10 wt.% [27]. A commercial Ni/Al_2O_3 catalyst doped with Ca (Süd

159 Chemie-G90LDP) was used in the reforming step, with its main properties being
160 reported in previous studies [44].

161 According to the scheme showed in Figure 1, steam was injected to the pyrolysis reactor
162 as fluidizing agent. It should be noted that it does not take part in the pyrolysis reaction,
163 as low temperatures were used (500 ºC). The produced pyrolysis volatiles (gaseous
164 products and bio-oil) were fed in line into the FBR for their reforming. The product
165 stream leaving the reformer was analyzed in line by gas chromatography (Agilent 6890
166 GC and Varian 4900 micro GC). The detailed experimental procedure and the analytical
167 techniques were detailed elsewhere [27].

168 The experiments were carried out in continuous regime under the following conditions:
169 biomass feed-rate, 0.75 g min^{-1}; pyrolysis step temperature, 500 ºC; steam reforming
170 temperature, between 550 and 700 ºC; steam/biomass (S/B) ratio, 2-5 range, and; space
171 time in the steam reforming step, 2-30 g_{cat} min g^{-1}. A previous experimental study of
172 biomass pyrolysis-reforming showed that a space time of 20 g_{cat} min g_{vol}^{-1} was required
173 to attain almost full conversion of pyrolysis volatiles [27]. Accordingly, these results
174 were considered for comparison with the simulated ones, as they were obtained mainly
175 under thermodynamic control. Thus, operating at 600 ºC with a S/B ratio of 4,
176 conversion was 99.7 % with a space time of 20 g_{cat} min g_{vol}^{-1}. A reduction in space time
177 progressively decreased the conversion in the reforming reaction and changed the
178 reaction control from thermodynamic to kinetic one.

179 **3. Results**

180 3.1. Validation of the simulation under SR conditions

181 H_2 yield and steam conversion are the reaction indexes in order to assess the
182 experimental results and validate the thermodynamic study of pyrolysis volatile

conversion. Volatile conversion (%) was defined as the ratio between the moles of C obtained in the gaseous product and those fed into the reforming step:

$$X = \frac{C_{gas}}{C_{volatiles}} \cdot 100 \quad (9)$$

It should be noted that the carbon contained in the pyrolysis char was not considered for estimating the reforming step conversion, as it was continuously withdrawn from the pyrolysis reactor.

The H_2 yield (wt.%) was calculated as the ratio between the H_2 mass flow rate (kg_{H2} min^{-1}) in the product stream (m_{H2}) and that of biomass in the feed ($kg_{biomaas}$ min^{-1}) into the pyrolysis step ($m_{biomass}$):

$$Y_{H_2} = \frac{m_{H_2}}{m_{biomass}} \cdot 100 \quad (10)$$

Steam conversion (%) was calculated considering the steam fed into the pyrolysis process and that reacted in the reforming step:

$$X_{H_2O} = 1 - \frac{m_{H_2O}}{m^0_{H_2O}} \cdot 100 \quad (11)$$

where m_{H_20} and $m^0{}_{H_20}$ (kg_{H2O} min^{-1}) are the steam mass flow rates in the reformer outlet and inlet, respectively.

The experimental results and those obtained by simulation in the steam reforming (ER = 0) at different temperatures are compared in Figure 3. The results correspond to a S/B ratio of 4 and a space time of 20 g_{cat} min g_{vol}^{-1}. As observed, the simulated results of both conversion and H_2 production are consistent with the experimental ones, with the exception of those obtained at 550 ° C. This is explained by the fact that conversion at 550 ºC was far from full (58.3%) due to the low reforming reaction rate at this

temperature. Therefore, this result under kinetic control was not considered in this simulation corresponding to equilibrium conditions.

An increase in temperature promotes the displacement of endothermic reforming reactions involving methane (Eq. 1), oxygenates (Eq. 2) and other hydrocarbons, which favor the conversion of biomass pyrolysis volatiles to H_2 and CO. However, an increase in temperature also shifts the equilibrium of the exothermic WGS reaction (Eq. 3). Thus, a slight decrease in hydrogen production was observed in both the experimental and calculated results at temperatures above 600 ºC. Similar results have been reported in the literature, wherein the influence of temperature in the reforming of biomass pyrolysis volatiles and raw bio-oil were analyzed [31,38,49,50].

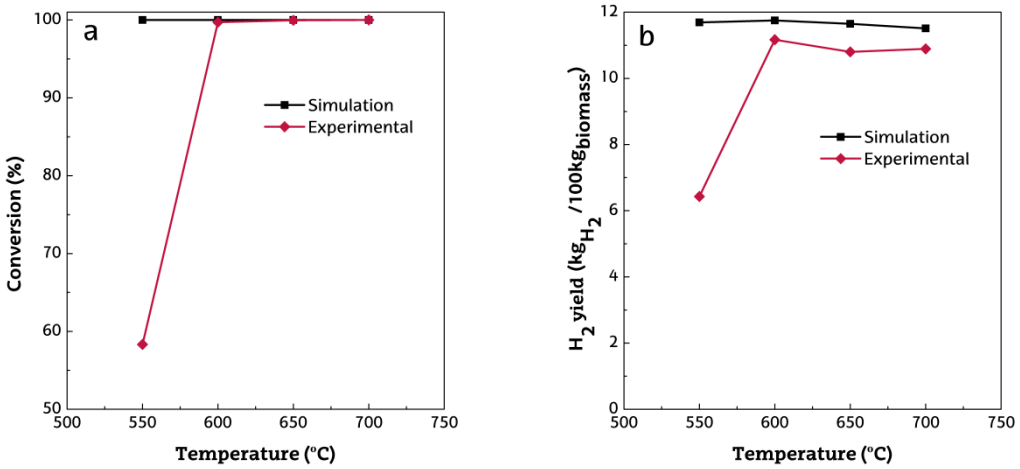

Figure 3. Comparison of simulated and experimental results of conversion (a) and H_2 yield (b) in the steam reforming (ER = 0) of biomass fast pyrolysis volatiles at different temperatures. S/B, 4; space time 20 g_{cat} min g_{vol}^{-1}.

The influence of S/B ratio on the experimental and calculated conversions and hydrogen yields is shown in Figure 4. As observed, the predictions based on thermodynamics are reasonably consistent with the experimental ones. The experimental conversions and hydrogen yields are slightly lower than those obtained by simulation. The differences

are explained by the gas bypass that inevitably occurs in fluidized bed reactors, which is associated with the gas fraction that crosses the bed in the bubble phase (leading to a poorer contact of the gas phase with the catalyst). Interestingly, the simulation results accurately predict the increase in hydrogen production with S/B, which is due to the displacement of the equilibrium in the WGS reaction (Eq. 3). The same effect of S/B ratio on hydrogen production was reported in the literature in the reforming of bio-oil and biomass pyrolysis volatiles [30,51-53].

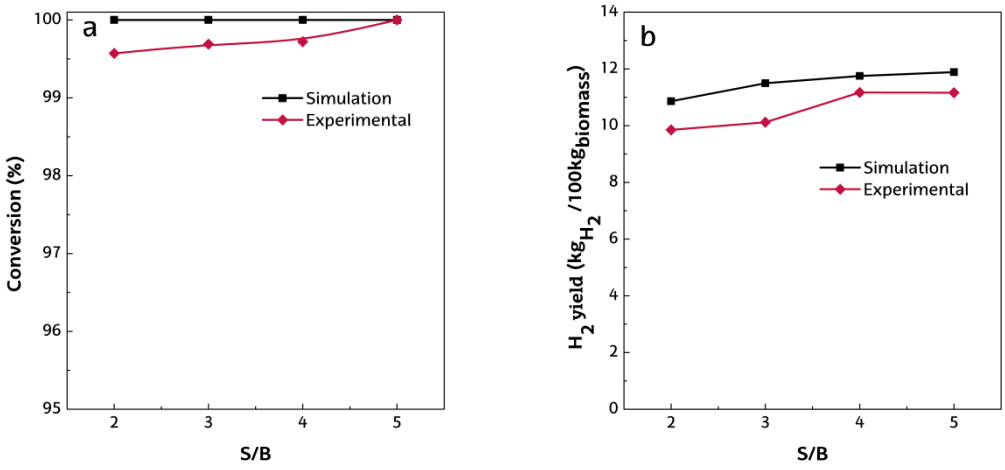

Figure 4. Comparison of the experimental results of conversion (a) and H_2 yield (b) with those obtained by simulation in the steam reforming (ER = 0) of biomass fast pyrolysis volatiles with different S/B ratios. 600 ºC; space time, 20 g_{cat} min g_{vol}^{-1}.

The afore mentioned good agreement between experimental and calculated SR results in a wide range of temperatures and S/B ratios is evidence of the validity of the simulation tool to predict OSR results and adjust operating conditions. It should be remarked that the applicability of the results is restricted to thermodynamic equilibrium conditions, i.e., high space times and reactions rates with no kinetic control.

3.2. Simulation of the OSR of biomass pyrolysis volatiles

The aim of this section is to evaluate the influence of the main OSR operating conditions, as are temperature, S/B ratio and ER, on gas product composition, hydrogen production and reaction enthalpy. This knowledge is essential for the fine-tuning of OSR conditions in future experimental studies.

Figure 5 shows the influence ER has on the composition of the gas product (on a dry basis) and steam conversion (Figure 5a), and on the reaction enthalpy (Figure 5b), at 700 ºC and S/B ratio of 2. A similar effect of ER was observed in the simulations performed at other temperatures and S/B ratios. Thus, an increase in ER caused an increase in CO_2 concentration and a reduction in those of hydrogen and CO. Thus, on the one hand, oxygen enhances combustion reactions, with the subsequent increase in CO_2 and H_2O concentrations, and reduces the extent of reforming reactions, which also leads to a reduction in H_2O conversion. On the other hand, a higher steam partial pressure in the reaction environment displaces the WGS equilibrium and modifies CO_2/CO balance. Finally, the relatively high temperature in this simulation, 700 ºC, ensures almost full CH_4 conversion.

Moreover, an increase in ER also modifies the reaction enthalpy, as observed in Figure 5b. The reaction is clearly endothermic operating with ER = 0 (ΔH_r= 2000 kJ/$kg_{biomass}$ at 700 ºC and S/B = 2), but autothermal reforming (ATR) conditions are attained with an ER of 0.135, and the reaction is highly exothermic (ΔH_r= -1100 kJ/$kg_{biomass}$) with an ER of 0.2. This evolution is explained by the increasing contribution of exothermic oxidation reactions as ER is raised and, to a minor extent, by the attenuation of reforming and WGS reactions.

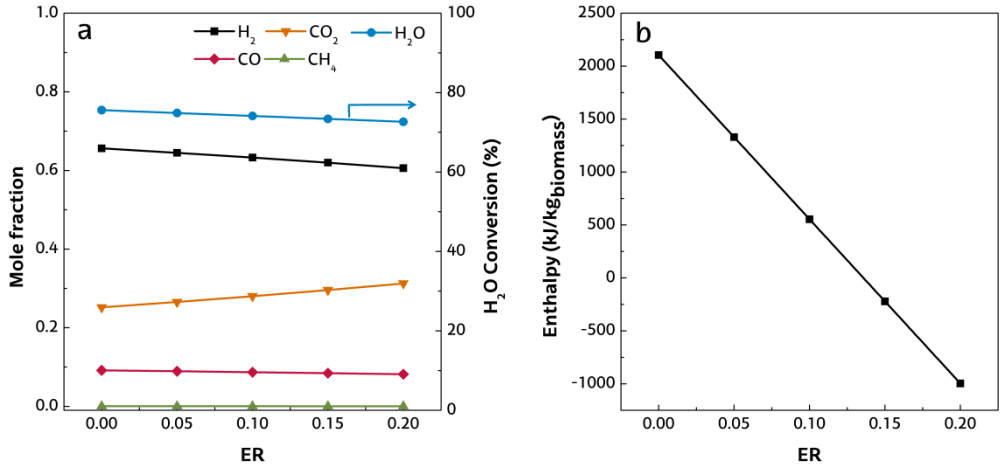

Figure 5. Evolution with ER of the gaseous product molar fraction (on a dry basis) and H_2O conversion (5a), and of reaction enthalpy (5b). 700 ºC; S/B ratio, 2.

Steam partial pressure is one of the most influential parameters in reforming processes, as it determines the steam reforming reaction rate and WGS reaction equilibrium, and contributes to attenuating catalyst deactivation by promoting coke gasification [54-56]. However, the use of an excessive steam flow rate in the reforming process significantly increases energy demand [30]. Operation under OSR conditions may reduce the optimum S/B ratio, as oxygen contributes to both feed conversion to CO_2 and combustion of coke deposits. Therefore, the evaluation of S/B ratio influence under OSR conditions is of great relevance.

Figure 6 shows the effect S/B ratio has on the gas product composition and water conversion at 700 ºC with an ER of 0.1 (Figure 6a). An increase in the steam concentration in the reaction environment shifts the WGS (Eq. 3) reaction equilibrium, thereby raising H_2 and CO_2 concentrations, whereas those of CO and CH_4 are remarkably reduced. As expected, water conversion decreases as its content in the feed is increased due to the limited impact of the excess steam on reforming (Eqs. 1 and 2) and WGS (Eq. 3) reactions when operating with high S/B ratios. It should be pointed

out that, although no additional steam was injected in the simulation performed with S/B = 0, bio-oil contains around 33 wt.% water (see Table 1) and, furthermore, oxygen (ER = 0.1) also promotes H_2O formation via combustion reactions (Eqs. 6-8). Accordingly, even under S/B = 0 conditions, SR reactions took place and CH_4 and CO are partially converted, thus attaining high H_2 concentrations.

As observed in Figure 6b for the simulation performed at 700 ºC with an ER ratio of 0.1, S/B ratio has a remarkable influence on the reforming step energy demand. As already mentioned, the results obtained with S/B = 0 are explained by the H_2O formed during both biomass pyrolysis and combustion reactions in the reforming step. An increase in S/B ratio to 0.5 leads to a sharp increase in reaction enthalpy due the enhancement of endothermic reforming reactions by the H_2O available in the reaction environment. However, a further increase in H_2O content in the reaction environment promotes the exothermic WGS reaction (Eq. 3) because the reforming reactions are fully shifted, as observed by monitoring the evolution of CO/CO_2 concentration and water conversion with S/B ratio (Figure 6a).

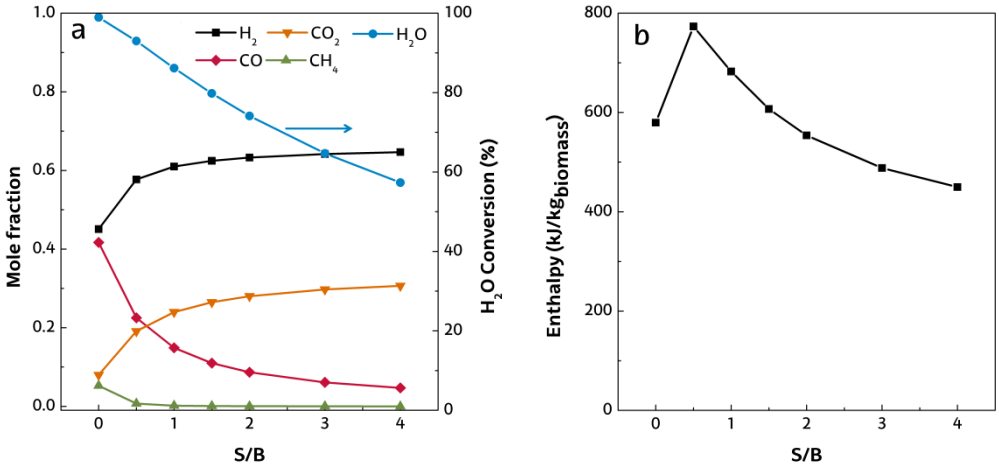

Figure 6. Evolution with S/B of the gaseous product molar fraction (on a dry basis) and H_2O conversion (6a), and of reaction enthalpy (6b). 700 ºC; ER, 0.1.

Temperature has also a great influence on the performance of the reforming process, as the endothermic reactions in this process require high temperatures to attain high reaction rates. Moreover, operation at higher temperature has a positive effect on catalyst deactivation in the SR of hydrocarbons and oxygenates, as it attenuates coke deposition [56-59]. However, the selection of the reforming temperature is also conditioned by catalyst stability, especially to avoid sintering phenomena, as well as energy requirements.

The reforming temperature has a remarkable effect on gas composition (Figure 7a). A high CH_4 concentration was observed at 500 ºC, which is evidence that its reforming is far from being complete. Temperatures higher than 800-900 ºC are usually required to ensure CH_4 full conversion [60,61], as this parameter strongly depends on the reaction environment composition, especially on the steam partial pressure [62]. An increase in temperature to 600 ºC enhances CH_4 reforming, which in turn increases H_2 concentration. However, an increase in temperature has also a negative effect on the WGS reaction equilibrium, which leads to higher CO concentrations and lower of those corresponding to H_2 and CO_2. This effect is evident above 600 ºC, leading to a significant reduction in hydrogen concentration. The mentioned effect of temperature on the extent of reforming and WGS reactions is also evident on H_2O conversion, which increases with temperature up to 600 ºC due to the promotion of reforming reaction rates. Nevertheless, a further increase in temperature reduces H_2O consumption by hindering WGS reaction.

Figure 7b shows that more energy is required in the reforming process as temperature is raised. Below 550 ºC, the process is exothermic due to both the low extent of endothermic reforming reactions and the contribution of exothermic WGS and

combustion ones. A further temperature increase to 600 ºC shifts the process to an energy demanding one, as reforming reactions are favored, whereas WGS is hindered.

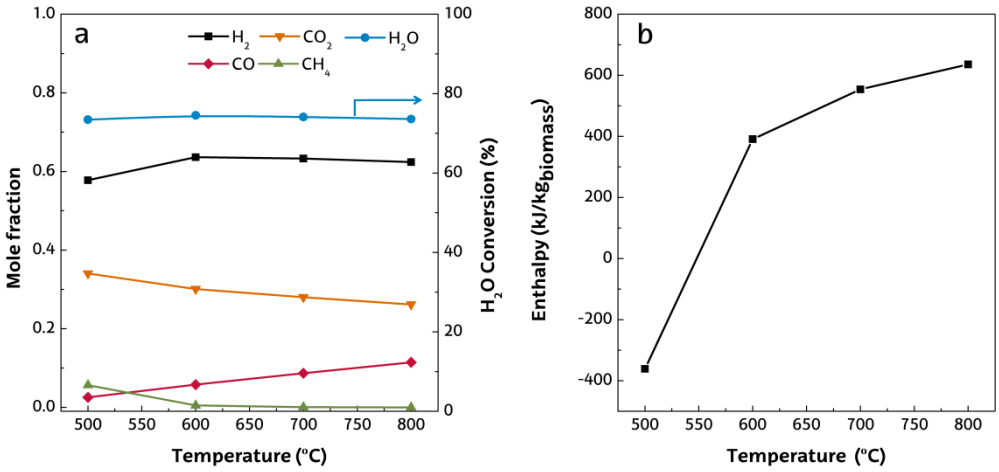

Figure 7. Evolution with temperature of the gaseous product molar fraction (on a dry basis) and H_2O conversion (7a), and of reaction enthalpy (7b). S/B ratio, 2; ER, 0.1.

Hydrogen production is the key objective for the determination of the most suitable reforming conditions. Figure 8 summarizes the combined influence of temperature, S/B ratio and ER on hydrogen yield in the OSR of biomass fast pyrolysis volatiles. As observed, hydrogen yields higher than 11 wt.% (by mass unit of biomass fed into the pyrolysis step) are obtained under suitable conditions; that is, temperatures between 600 and 700 ºC, S/B ratios higher than 2 and without oxygen (ER = 0). Figures 8a and 8c show that temperature should be higher than 580 ºC to enhance reforming reactions, but values above 700 ºC decrease hydrogen production by shifting in WGS reaction equilibrium. Other authors established similar optimum temperatures in thermodynamic studies involving the reforming of bio-oil and bio-oil model compounds [61,63-65]. An increase in S/B ratio clearly improves hydrogen production due to the shift of the WGS reaction, especially when the process is carried out in the optimum temperature range (Figure 8c). Therefore, S/B ratio should be carefully selected because values above 2

allow attaining only a slight increase in hydrogen production (Figures 8b and 8c) at the expense of a remarkable increase in the energy demand of the process. Finally, an increase in ER causes a reduction in hydrogen production (Figures 8a and 8b). It is noteworthy that the ER required to attain autothermal operation is of around 0.13, with the maximum hydrogen production being slightly lower than 10 wt.% under these conditions.

Therefore, operation under suitable conditions allow obtaining high hydrogen yields and avoiding the limitations associated with the severe endothermicity of the conventional SR process. It is noteworthy that alternative processes for hydrogen production from biomass, such as steam gasification, lead to considerably lower yields. Thus, operating under suitable process conditions and using an efficient in situ catalysts (such as dolomite, ɣ-Al_2O_3 or olivine), hydrogen yields in the 5 to 8 wt.% range are commonly reported in the steam gasification in fluidized and spouted bed reactors [66-69]. In addition, the hydrogen productions obtained in the indirect route of biomass fast pyrolysis and bio-oil reforming are of the same order or slightly lower than those obtained in the direct biomass pyrolysis-reforming process proposed in the current study [3,54,59,70].

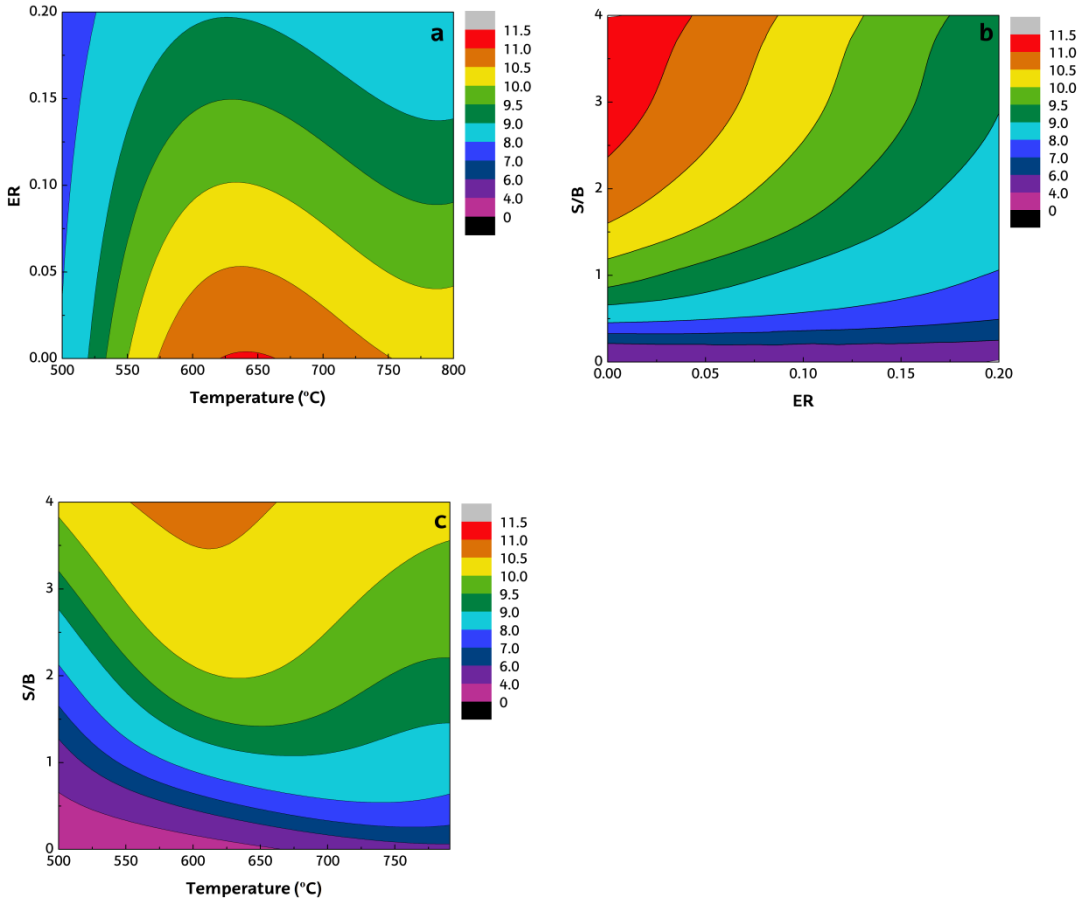

Figure 8. Combined effect of operating conditions on hydrogen yield (kg/100 kg of biomass) in the OSR of biomass fast pyrolysis volatiles. Effect of ER and temperature at S/B = 2 (a). Effect of S/B and ER at 700 ºC (b). Effect of S/B and temperature at ER = 0.1 (c).

3.3. ER values for autothermal operation under different process conditions

In the previous section it was determined that the ER value to attain autothermal operation ($\Delta Hr = 0$) is of 0.135 operating at 700 ºC with an S/B ratio of 2 (Figure 5). However, ER strongly depends on operating conditions; therefore, this section deals the influence temperature and S/B ratio have on the ER required to attain autothermal reforming (ATR) conditions. In addition, hydrogen yields obtained under ATR and SR

conditions are compared to determine the potential of the process and the most suitable operating conditions.

Figure 9 summarizes the influence of S/B ratio and temperature on the ER for autothermal operation. As observed in Figure 9a, the ER values required to operate at 500 °C with S/B values of 0 and 0.5 are negative, which obviously has no physical meaning. The ER values obtained are explained by the steam partial pressure attained in the reactor under these conditions. Thus, when operating with S/B = 0, steam partial pressure is very low (only that associated with moisture content and formed in the biomass pyrolysis). Accordingly, steam reforming reactions hardly occur due to both their endothermicity and the low steam partial pressure. As temperature is increased, the steam in the reaction environment is consumed in the reforming reactions, with no water for the exothermic WGS reaction. This fact leads to an increase in the endothermicity of the overall reaction, which in turn increases the ER value required for ATR operation. This increase in ER promotes CO_2 formation, and therefore endothermic dry reforming reactions (Eqs. 4 and 5), which contribute to increasing reaction enthalpy.

High S/B ratios increase steam concentration, which enhances reforming reactions at low temperatures and so the endothermic nature of the process, thereby increasing the ER value required for attaining ATR operation. However, when operating at high temperatures, S/B ratio showed an opposite effect on the autothermal ER value, as the extent of the exothermic WGS reaction strongly depends on steam partial pressure. Thus, high S/B ratios shift the WGS reaction, and so reduce the ER values required for ATR operation.

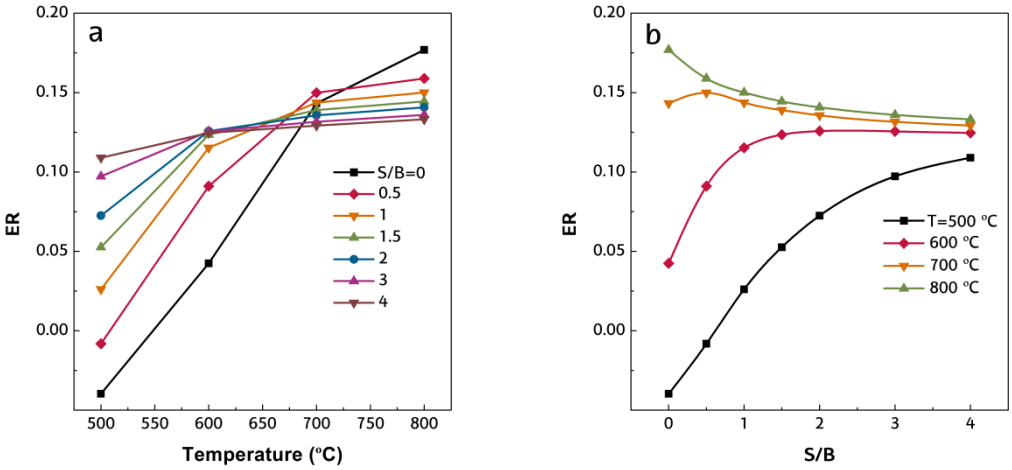

391

392 **Figure 9.** Effect of temperature (9a) and S/B ratio (9b) on the ER under
393 autothermal conditions for different S/B ratios and temperatures, respectively.

394

395 Figure 10 compares the hydrogen yields obtained under autothermal and SR conditions
396 at different temperatures and S/B ratios. As observed, the highest hydrogen yields are
397 obtained at 600 ºC with high S/B ratios. However, there is hardly any improvement for
398 S/B ratios higher than 2, i.e., from 9.7 wt.% with S/B = 2 to 10.4 wt.% with S/B = 4,
399 and therefore a S/B value of 2 is suitable from the perspective of efficiency.
400 Interestingly, when operating at 600 ºC with a S/B ratio of 2, the hydrogen yield under
401 ATR conditions is only 12 % lower than under SR conditions, whereas at 700 and 800
402 ºC this reduction is of 15 and 16 %, respectively. This result is explained by the
403 significantly lower ER required for attaining ATR operation at 600 ºC (see Figure 9b),
404 which improves the hydrogen production potential at this temperature. Accordingly,
405 temperatures between 600 and 700 ºC and S/B ratios between 2 and 3 are the most
406 suitable conditions for the OSR reforming of biomass pyrolysis volatiles under ATR
407 conditions. These results should be confirmed in future studies by conducting
408 experiments in a range of process conditions. Furthermore, optimization of process

409 conditions should also consider catalyst deactivation, since previous studies dealing
410 with the reforming of biomass derivatives revealed a notable influence of operating
411 conditions (especially temperature and S/B ratio) on the catalyst deactivation
412 mechanism (coke formation, and its nature, evolution and in situ gasification) and
413 deactivation rate [51,52,55,56,71].

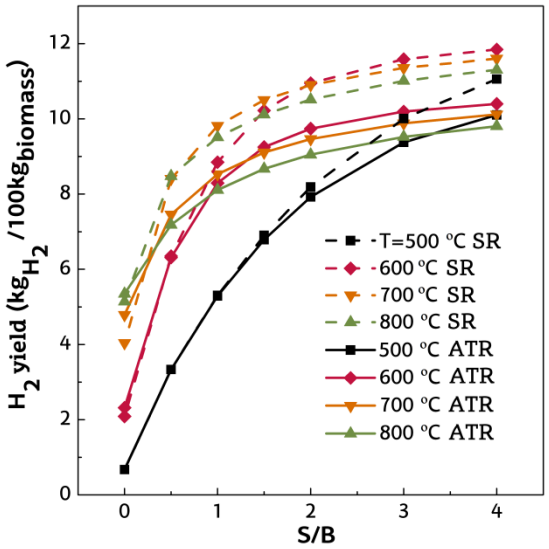

414

415 **Figure 10.** Comparison of hydrogen yield values obtained at different temperatures
416 and S/B ratios under ATR and SR (ER = 0) conditions.

417 3.4. Discussion and comparison with other technologies for H_2 production from
418 biomass

419 Several strategies have been proposed in the literature for H_2 production from biomass.
420 In this work, the great potential of biomass pyrolysis and oxidative steam reforming (P-
421 OSR) was proven. The co-feeding of oxygen with steam in the reaction system allows
422 the provision of additional energy for the endothermic reforming reactions [17] and,
423 moreover, the gasification of the coke deposited on the catalyst is also promoted, which
424 potentially improves catalyst stability [20,22]. Thus, Table 4 summarizes the results

obtained in this study and in other similar literature results regarding oxidative and autothermal reforming (OSR and ATR, respectively), as well as those obtained with other thermochemical process for biomass conversion to H_2, such as steam reforming (SR) or steam gasification (SG).

It is to note that although the advantages of the oxidative steam reforming have attracted increasing attention in the literature for oxygenated compounds [25,72,73], there are hardly studies conducted with raw bio-oil [74-76]. Besides, the main limitation of this process compared to the conventional SR one is the lower H_2 yield obtained when O_2 is co-fed in the OSR [17,77,78]. Consequently, numerous experimental and thermodynamic analyses have been carried out in order to establish the optimum operating conditions and compensate this lower yield with higher catalyst stability. As observed in Table 4, Vagia et al. [17] conducted a thermodynamic analysis of the autothermal steam reforming of selected compounds of the bio-oil (acetic acid, acetone and ethylene glycol). They concluded that the highest H_2 yield was obtained at 627 ºC, with the optimum amount of oxygen being highly dependent on the steam/fuel ratio and the type of oxygenate compound used. However, they observed a hydrogen yield of around 20% lower than the one obtained by steam reforming, since part of the organic feed is consumed in the combustion reaction. Czernik and French [74] obtained similar results of H_2 production than the ones reported in this study, demonstrating the technical viability of hydrogen production by auto-thermal reforming of fast pyrolysis bio-oils produced from three biomass feedstocks. The OSR of raw bio-oil was also studied by Remiro et al. [76] using a Rh-CeO_2-ZrO_2 catalyst. In this case, the H_2 production by mass unit of the raw bio-oil was lower than in the two-stage process studied here, since a H_2 fraction is lost as pyrolytic lignin in the volatilization of the bio-oil prior to feed into the reforming reactor.

It is to note that H_2 production in a two-step process of pyrolysis-oxidative steam reforming has been hardly analyzed in the literature. Thus, the group headed by Prof. Tomishige studied the pyrolysis-oxidative reforming in a laboratory-scale continuous feeding dual-bed reactor, in which the biomass is fed into the primary bed, and pyrolysis volatiles are driven to the second step. However, they reported total loss of catalyst activity due to oxidation of the active Ni metal particles when they tested a Ni/Mg/Al catalyst [79]. The comparison of OSR literature studies with those of the SR process revealed that the selection of suitable operating conditions could lead to similar H_2 productions.

In addition, several literature results regarding biomass steam gasification were also summarized in Table 4. It is noteworthy that this alternative process for H_2 production from biomass leads to considerably lower yields (in the range from 3 to 8wt.%), even when primary catalysts, such as dolomite or olivine, are used in the gasification reactor [80-82]. Moreover, the higher temperature required in this process, as well as the problems associated with the tar content and the quality of the syngas obtained, make the pyrolysis and in-line oxidative steam reforming a promising solution for H_2 production from biomass. In view of the afore mentioned results, it can be concluded that the two-step process of pyrolysis and in-line OSR is a promising route for H_2 production from biomass, as it allows obtaining high hydrogen productions with several operational advantages. However, a further development of this process requires detailed studies in specific areas, such as catalyst design, deactivation-regeneration and technical development.

472 **Table 4** Summary of different strategies for H_2 production from biomass reported in the literature.

Kind of study	**Reactor configuration**	**Process**	**Raw material**	**Catalyst**	**Operating conditions**	**H_2 conc. (vol.%)**	**H_2 prod. (wt.%)[a]**	**Ref.**
Thermodynamic study	Gibbs reactor	P-OSR	Pine wood	-	TR = 500-800 ºC S/B = 0-4 ER = 0-0.2	66	10	This study
Experimental	Packed-bed reformer / WGS reactor	OSR	Oak, poplar and pine bio-oil	Commercial Pt/Al_2O_3	$GC_1HSV = 2000\ h^{-1}$ T = 800-850 ºC	65	11	[74]
				Commercial Fe/Cr catalyst (WGS)	S/C = 2.8-4 O/C = 0.9-1.1			
Thermodynamic and experimental study Pilot installation (1.5 kg h-1)	Fixed bed	ATR	Pine wood bio-oil	Ni-monolith	ER = 0.25-0.42	38	6.4	[75]
				Pt-Rh-Pd-monolith	S/C = 1.2-2			
Thermodynamic study	Gibbs reactor	ATR	Bio-oil model compounds (acetic acid, acetone and ethylene glycol)	-	TR = 127-1027 ºC S/F ratio = 1-9 P = 1-20 atm	65	13.6	[17]

Laboratory scale (0.08 ml min^{-1})	Fixed bed/ fluidized bed	OSR	Raw bio-oil	Rh-CeO_2-ZrO_2	T = 650-750 ºC S/C = 3-9 O/C = 0.34 ST = 0.15-0.6 $g_{cat}/g_{bio-oil}$		4.5[c]	[76]
Laboratory scale (150 mg min^{-1})	Dual fixed bed	P-PO	Cedar wood	Ni/Al_2O_3, Ni/ZrO_2, Ni/TiO_2, Ni/CeO_2, Ni/MgO	T = 550-650 ºC ER = 0.25	36.7	3.8	[83]
Laboratory scale (60 mg min^{-1})	Dual fixed bed	P-OSR	Cedar wood	Pd on hydrotalcite-derived Ni/Mg/Al catalyst	T = 500-600 ºC S/C = 0.24 ER = 0.14	43.7	5.0	[79]
Bench scale (0.6–1.5 g min^{-1})	Spouted bed /fluidized bed	P-SR	Pine Wood sawdust	Commercial (G90 LDP)	T_P = 500 °C T_R = 550-700 °C S/C = 7.7	66.0	11.0	[27]
Bench scale (0.75 g min^{-1})	Spouted bed /fluidized bed	P-SR	Pine wood sawdust	Ni/Al_2O_3, Ni/MgO, Ni/SiO_2, Ni/TiO_2, Ni/ZrO_2	T_P = 500 °C T_R =600 °C S/C = 7.7	65.4	10.7	[33]
Laboratory scale	Dual fixed	P-SR	Cedar wood	Ni/Al_2O_3, Ni/ZrO_2, Ni/TiO_2, Ni/CeO_2,	T = 550-650 ºC	60.1	8.3	[83]

(60 mg min^{-1})	bed			Ni/MgO	S/C = 0.5			
Laboratory scale (0.1 ml min^{-1})	Fixed bed/ fluidized bed	SR	Bio-oil aqueous fraction	Ni/La_2O_3-αAl_2O_3	T_1 = 500 ºC T_2 = 600-800 ºC ST = 0.10-0.45 g_{cat} h g $_{biooil}$ S/C = 12		10.1[b] 15.6[c]	[59]
Laboratory scale (0.3 g min^{-1})	Fixed bed / fixed bed	SR	Corn stalk pyrolysis oil	Ni-Al modified with Ca, Ce, Mg, Mn and Zn	T_1= 400 ºC (volatilization) T_2= 600-900 ºC ST = 1.67 g_{cat} min $g_{bio\text{-}oil}^{-1}$ S/C= 3.54-9	57.2	10.4[c]	[84]
Bench scale (0.75-1.5 g min^{-1})	Conical Spouted Bed	SG	Pinewood sawdust	None	T = 800-900 ºC S/B = 0-2	38	3.3	[80]
Laboratory scale (5 g min^{-1})	Fixed bed	SG	Pine sawdust	*Primary:* Dolomite	T = 600-900 ºC S/B = 1.2	51	7.3	[81]
Demonstration plant (1.2 tn day^{-1})	Updraft fixed bed	SG	Pallets wood chips	None	T = 750 ºC S/B = 1.4-2.7	55	6.4	[82]
Pilot plant	Rotary kiln	SG	Palm	None	T = 850 ºC	52	3.7	[85]

(3-4 kg h^{-1})			shells		S/B = 0.6-1			
Pilot plant (4 kg h^{-1})	Bubbling fluidized bed	SG	Pinewood chips	None	T = 750-780 ºC S/B = 0.53-1.1	56	6.9	[86]

[a] H_2 production defined as g_{H2}/100 $g_{biomass}$

[b] H_2 production defined as g_{H2}/100 $g_{bio\text{-}oil.}$

[c] Calculated based on H_2 yield and bio-oil composition.

Conclusions

The effect oxygen addition has on the reforming of biomass fast pyrolysis volatiles was simulated using thermodynamic equilibrium approach based on the Gibbs free energy minimization method. A detailed study was carried out of the influence temperature, steam/biomass (S/B) ratio and equivalence ratio (ER) have on hydrogen production and reaction enthalpy. Moreover, the ER needed for operating under ATR conditions was also ascertained. The results obtained in this simulation were validated with experimental results under SR conditions obtained in a previous study. An ER of 0.12 is required to attain ATR operation under optimum reforming conditions, i.e., temperatures between 600 and 700 ºC and S/B ratios in the 2 to 3 range. Interestingly, hydrogen productions of around 10 wt.% can be obtained under these conditions, which means only 12% reduction of that attained under SR conditions (ER = 0). These encouraging results are evidence of the interest of fast pyrolysis and in line OSR, i.e., a high hydrogen production is ensured and energy supply to the reforming process is solved. However, experimental runs in future studies should confirm these results.

Acknowledgements

This work was carried out with the financial support from Spain's ministries of Economy and Competitiveness (CTQ2016-75535-R (AEI/FEDER, UE)) and Science, Innovation and Universities (RTI2018-101678-B-I00 (MCIU/AEI/FEDER, UE)), the Basque Government (IT1218-19), and the European Union's Horizon 2020 research and innovation program under the Marie Skłodowska-Curie grant agreement No. 823745.

References

[1] International Energy Agency (IEA) Technology roadmap: hydrogen and fuel cells. Paris. 2015.

[2] Pandey B, Prajapati YK, Sheth PN Recent progress in thermochemical techniques to produce hydrogen gas from biomass: A state of the art review. Int J Hydrogen Energy 2019;44:25384-415.

[3] Arregi A, Amutio M, Lopez G, Bilbao J, Olazar M Evaluation of thermochemical routes for hydrogen production from biomass: A review. Energy Convers Manage 2018;165:696-719.

[4] Heidenreich S, Foscolo PU New concepts in biomass gasification. Prog Energy Combust Sci 2015;46:72-95.

[5] Lopez G, Artetxe M, Amutio M, Alvarez J, Bilbao J, Olazar M Recent advances in the gasification of waste plastics. A critical overview. Renewable Sustainable Energy Rev 2018;82:576-96.

[6] Molino A, Chianese S, Musmarra D Biomass gasification technology: The state of the art overview. J Energy Chem 2016;25:10-25.

[7] Dou B, Zhang H, Song Y, et al. Hydrogen production from the thermochemical conversion of biomass: Issues and challenges. Sustain Energy Fuels 2019;3:314-42.

[8] Hosseini SE, Abdul Wahid M, Jamil MM, Azli AAM, Misbah MF A review on biomass-based hydrogen production for renewable energy supply. Int J Energy Res 2015;39:1597-615.

[9] Nabgan W, Tuan Abdullah TA, Mat R, et al. Renewable hydrogen production from bio-oil derivative via catalytic steam reforming: An overview. Renewable Sustainable Energy Rev 2017;79:347-57.

[10] Guan G, Kaewpanha M, Hao X, Abudula A Catalytic steam reforming of biomass tar: Prospects and challenges. Renewable Sustainable Energy Rev 2016;58:450-61.

[11] Claude V, Courson C, Köhler M, Lambert SD Overview and Essentials of Biomass Gasification Technologies and Their Catalytic Cleaning Methods. Energy Fuels 2016;30:8791-814.

[12] Font Palma C Modelling of tar formation and evolution for biomass gasification: A review. Appl Energy 2013;111:129-41.

[13] Ayalur Chattanathan S, Adhikari S, Abdoulmoumine N A review on current status of hydrogen production from bio-oil. Renewable Sustainable Energy Rev 2012;16:2366-72.

[14] Chen J, Sun J, Wang Y Catalysts for Steam Reforming of Bio-oil: A Review. Ind Eng Chem Res 2017;56:4627-37.

[15] Valle B, Remiro A, García-Gómez N, Gayubo AG, Bilbao J Recent research progress on bio-oil conversion into bio-fuels and raw chemicals: a review. J Chem Technol Biotechnol 2019;94:670-89.

[16] Bridgwater AV Review of fast pyrolysis of biomass and product upgrading. Biomass Bioenergy 2012;38:68-94.

[17] Vagia EC, Lemonidou AA Thermodynamic analysis of hydrogen production via autothermal steam reforming of selected components of aqueous bio-oil fraction. Int J Hydrogen Energy 2008;33:2489-500.

[18] Cai W, Wang F, Zhan E, Van Veen AC, Mirodatos C, Shen W Hydrogen production from ethanol over Ir/CeO2 catalysts: A comparative study of steam reforming, partial oxidation and oxidative steam reforming. J Catal 2008;257:96-107.

[19] Cui X, Kær SK Thermodynamic analysis of steam reforming and oxidative steam reforming of propane and butane for hydrogen production. Int J Hydrogen Energy 2018;43:13009-21.

[20] Trane-Restrup R, Jensen AD Steam reforming of cyclic model compounds of bio-oil over Ni-based catalysts: Product distribution and carbon formation. Appl Catal , B 2015;165:117.

[21] Modafferi V, Panzera G, Baglio V, Frusteri F, Antonucci PL Propane reforming on Ni–Ru/GDC catalyst: H2 production for IT-SOFCs under SR and ATR conditions. Appl Catal A Gen 2008;334:1-9.

[22] Nahar G, Dupont V Recent advances in hydrogen production via autothermal reforming process (ATR): A review of patents and research articles. Recent Pat Chem Eng 2013;6:8-42.

[23] Gaber C, Demuth M, Schluckner C, Hochenauer C Thermochemical analysis and experimental investigation of a recuperative waste heat recovery system for the tri-reforming of light oil. Energy Convers Manage 2019;195:302-12.

[24] Wang J, Chen H, Tian Y, Yao M, Li Y Thermodynamic analysis of hydrogen production for fuel cells from oxidative steam reforming of methanol. Fuel 2012;97:805-11.

[25] Nahar GA, Madhani SS Thermodynamics of hydrogen production by the steam reforming of butanol: Analysis of inorganic gases and light hydrocarbons. Int J Hydrogen Energy 2010;35:98-109.

[26] Montero C, Oar-Arteta L, Remiro A, Arandia A, Bilbao J, Gayubo AG Bilbao, J.; Gayubo, A. G. Thermodynamic comparison between bio-oil and ethanol steam reforming. Int J Hydrogen Energy 2015;40:15963.

[27] Arregi A, Lopez G, Amutio M, Barbarias I, Bilbao J, Olazar M Hydrogen production from biomass by continuous fast pyrolysis and in-line steam reforming. RSC Adv 2016;6:25975-85.

[28] Cao J, Shi P, Zhao X, Wei X, Takarada T Catalytic reforming of volatiles and nitrogen compounds from sewage sludge pyrolysis to clean hydrogen and synthetic gas over a nickel catalyst. Fuel Process Technol 2014;123:34-40.

574 [29] Cao J, Liu T, Ren J, et al. Preparation and characterization of nickel loaded on resin
575 char as tar reforming catalyst for biomass gasification. J Anal Appl Pyrolysis
576 2017;127:82-90.

577 [30] Xiao X, Meng X, Le DD, Takarada T Two-stage steam gasification of waste
578 biomass in fluidized bed at low temperature: Parametric investigations and performance
579 optimization. Bioresour Technol 2011;102:1975-81.

580 [31] Xiao X, Cao J, Meng X, et al. Synthesis gas production from catalytic gasification
581 of waste biomass using nickel-loaded brown coal char. Fuel 2013;103:135-40.

582 [32] Santamaria L, Arregi A, Alvarez J, et al. Performance of a Ni/ZrO2 catalyst in the
583 steam reforming of the volatiles derived from biomass pyrolysis. J Anal Appl Pyrolysis
584 2018;136:222-31.

585 [33] Santamaria L, Lopez G, Arregi A, et al. Influence of the support on Ni catalysts
586 performance in the in-line steam reforming of biomass fast pyrolysis derived volatiles.
587 Appl Catal B Environ 2018;229:105-13.

588 [34] Yu H, Liu Y, Liu J, Chen D High catalytic performance of an innovative
589 Ni/magnesium slag catalyst for the syngas production and tar removal from biomass
590 pyrolysis. Fuel 2019;254:115622.

591 [35] Chai Y, Gao N, Wang M, Wu C H2 production from co-pyrolysis/gasification of
592 waste plastics and biomass under novel catalyst Ni-CaO-C. Chem Eng J
593 2020;382:122947.

594 [36] Barbarias I, Lopez G, Alvarez J, et al. A sequential process for hydrogen
595 production based on continuous HDPE fast pyrolysis and in-line steam reforming.
596 Chem Eng J 2016;296:191-8.

597 [37] Barbarias I, Lopez G, Artetxe M, Arregi A, Bilbao J, Olazar M Valorisation of
598 different waste plastics by pyrolysis and in-line catalytic steam reforming for hydrogen
599 production. Energy Convers Manage 2018;156:575-84.

600 [38] Arregi A, Amutio M, Lopez G, et al. Hydrogen-rich gas production by continuous
601 pyrolysis and in-line catalytic reforming of pine wood waste and HDPE mixtures.
602 Energy Convers Manag 2017;136:192-201.

603 [39] Alvarez J, Lopez G, Amutio M, et al. Characterization of the bio-oil obtained by
604 fast pyrolysis of sewage sludge in a conical spouted bed reactor. Fuel Process Technol
605 2016;149:169-75.

606 [40] Alvarez J, Hooshdaran B, Cortazar M, et al. Valorization of citrus wastes by fast
607 pyrolysis in a conical spouted bed reactor. Fuel 2018;224:111-20.

608 [41] Moliner C, Marchelli F, Bosio B, Arato E Modelling of spouted and spout-fluid
609 beds: Key for their successful scale up. Energies 2017;10:1729.

[42] Lopez G, Artetxe M, Amutio M, Bilbao J, Olazar M Thermochemical routes for the valorization of waste polyolefinic plastics to produce fuels and chemicals. A review. Renewable Sustainable Energy Rev 2017;73:346-68.

[43] Perkins G, Bhaskar T, Konarova M Process development status of fast pyrolysis technologies for the manufacture of renewable transport fuels from biomass. Renewable Sustainable Energy Rev 2018;90:292-315.

[44] Erkiaga A, Lopez G, Barbarias I, et al. HDPE pyrolysis-steam reforming in a tandem spouted bed-fixed bed reactor for H2 production. J Anal Appl Pyrolysis 2015;116:34-41.

[45] Lan P, Xu Q, Zhou M, Lan L, Zhang S, Yan Y Catalytic steam reforming of fast pyrolysis bio-oil in fixed bed and fluidized bed reactors. Chem Eng Technol 2010;33:2021-8.

[46] Park Y, Namioka T, Sakamoto S, Min Tj, Roh Sa, Yoshikawa K Optimum operating conditions for a two-stage gasification process fueled by polypropylene by means of continuous reactor over ruthenium catalyst. Fuel Process Technol 2010;91:951-7.

[47] Wu C, Williams PT Pyrolysis-gasification of plastics, mixed plastics and real-world plastic waste with and without Ni-Mg-Al catalyst. Fuel 2010;89:3022-32.

[48] Amutio M, Lopez G, Artetxe M, Elordi G, Olazar M, Bilbao J Influence of temperature on biomass pyrolysis in a conical spouted bed reactor. Resour Conserv Recycl 2012;59:23-31.

[49] Koike M, Ishikawa C, Li D, Wang L, Nakagawa Y, Tomishige K Catalytic performance of manganese-promoted nickel catalysts for the steam reforming of tar from biomass pyrolysis to synthesis gas. Fuel 2013;103:122-9.

[50] Ma Z, Zhang S-, Xie D-, Yan Y- A novel integrated process for hydrogen production from biomass. Int J Hydrogen Energy 2014;39:1274-9.

[51] Remiro A, Valle B, Aguayo AT, Bilbao J, Gayubo AG Steam reforming of raw bio-oil in a fluidized bed reactor with prior separation of pyrolytic lignin. Energy Fuels 2013;27:7549-59.

[52] Lan P, Lan LH, Xie T, Liao AP The preparation of syngas by the reforming of bio-oil in a fluidized-bed reactor. Energy Sources Recovery Util Environ Eff 2014;36:242-9.

[53] Wu C, Huang Q, Sui M, Yan Y, Wang F Hydrogen production via catalytic steam reforming of fast pyrolysis bio-oil in a two-stage fixed bed reactor system. Fuel Process Technol 2008;89:1306-16.

[54] Garcia L, French R, Czernik S, Chornet E Catalytic steam reforming of bio-oils for the production of hydrogen: effects of catalyst composition. Appl Catal, A Gen 2000;201:225.

[55] Li H, Xu Q, Xue H, Yan Y Catalytic reforming of the aqueous phase derived from fast-pyrolysis of biomass. Renew Energy 2009;34:2872-7.

[56] Arregi A, Lopez G, Amutio M, et al. Role of operating conditions in the catalyst deactivation in the in-line steam reforming of volatiles from biomass fast pyrolysis. Fuel 2018;216:233-44.

[57] Efika CE, Wu C, Williams PT Syngas production from pyrolysis-catalytic steam reforming of waste biomass in a continuous screw kiln reactor. J Anal Appl Pyrolysis 2012;95:87-94.

[58] Nahil MA, Wang X, Wu C, Yang H, Chen H, Williams PT Novel bi-functional Ni-Mg-Al-CaO catalyst for catalytic gasification of biomass for hydrogen production with in situ CO2 adsorption. RSC Adv 2013;3:5583-90.

[59] Remiro A, Valle B, Aguayo AT, Bilbao J, Gayubo AG Operating conditions for attenuating Ni/La2O3-Al2O3 catalyst deactivation in the steam reforming of bio-oil aqueous fraction. Fuel Process Technol 2013;115:222-32.

[60] Pashchenko D Combined methane reforming with a mixture of methane combustion products and steam over a Ni-based catalyst: An experimental and thermodynamic study. Energy 2019;185:573-84.

[61] Soria MA, Barros D, Madeira LM Hydrogen production through steam reforming of bio-oils derived from biomass pyrolysis: Thermodynamic analysis including in situ CO2 and/or H2 separation. Fuel 2019;244:184-95.

[62] Yao X, Yu Q, Xie H, et al. The production of hydrogen through steam reforming of bio-oil model compounds recovering waste heat from blast furnace slag: Thermodynamic study. J Therm Anal Calor 2018;131:2951-62.

[63] Xie H, Li R, Wang Z, Yao X, Yu Q Hydrogen production of bio-oil steam reforming combining heat recovery of blast furnace slag: Thermodynamic analysis. Int J Hydrogen Energy 2019;44:25514-23.

[64] Saeed Baamran K, Tahir M Thermodynamic investigation and experimental analysis on phenol steam reforming towards enhanced H2 production over structured Ni/ZnTiO3 nanocatalyst. Energy Convers Manage 2019;180:796-810.

[65] Sahebdelfar S Steam reforming of propionic acid: Thermodynamic analysis of a model compound for hydrogen production from bio-oil. Int J Hydrogen Energy 2017;42:16386-95.

[66] Rapagna S, Virginie M, Gallucci K, et al. Fe/olivine catalyst for biomass steam gasification: Preparation, characterization and testing at real process conditions. Catal Today 2011;176:163-8.

[67] Cortazar M, Lopez G, Alvarez J, Amutio M, Bilbao J, Olazar M Behaviour of primary catalysts in the biomass steam gasification in a fountain confined spouted bed. Fuel 2019;253:1446-56.

686 [68] Michel R, Rapagn S, Di Marcello M, et al. Catalytic steam gasification of
687 Miscanthus X giganteus in fluidised bed reactor on olivine based catalysts. Fuel Process
688 Technol 2011;92:1169-77.

689 [69] Xie Y, Xiao J, Shen L, Wang J, Zhu J, Hao J Effects of Ca-based catalysts on
690 biomass gasification with steam in a circulating spout-fluid bed reactor. Energy Fuels
691 2010;24:3256-61.

692 [70] Bimbela F, Oliva M, Ruiz J, García L, Arauzo J Hydrogen production via catalytic
693 steam reforming of the aqueous fraction of bio-oil using nickel-based coprecipitated
694 catalysts. Int J Hydrogen Energy 2013;38:14476-87.

695 [71] Wang Z, Pan Y, Dong T, et al. Production of hydrogen from catalytic steam
696 reforming of bio-oil using C12A7-O--based catalysts. Appl Catal A Gen 2007;320:24-
697 34.

698 [72] Kamonsuangkasem K, Therdthianwong S, Therdthianwong A Hydrogen
699 production from yellow glycerol via catalytic oxidative steam reforming. Fuel Process
700 Technol 2013;106:695-703.

701 [73] Mondal T, Pant KK, Dalai AK Oxidative and non-oxidative steam reforming of
702 crude bio-ethanol for hydrogen production over Rh promoted Ni/CeO2-ZrO2 catalyst.
703 Appl Catal A Gen 2015;499:19-31.

704 [74] Czernik S, French R Distributed production of hydrogen by auto-thermal reforming
705 of fast pyrolysis bio-oil. Int J Hydrogen Energy 2014;39:744-50.

706 [75] Leijenhorst EJ, Wolters W, Van de Beld L, Prins W Autothermal catalytic
707 reforming of pine wood derived fast pyrolysis-oil in a 1.5kg/h pilot installation: Aspects
708 of adiabatic operation. Fuel Process Technol 2013;115:164-73.

709 [76] Remiro A, Arandia A, Oar-Arteta L, Bilbao J, Gayubo AG Stability of a Rh/CeO2-
710 ZrO2 Catalyst in the Oxidative Steam Reforming of Raw Bio-oil. Energy Fuels
711 2018;32:3588-98.

712 [77] Trane R, Dahl S, Skjoth-Rasmussen MS, Jensen AD Catalytic steam reforming of
713 bio-oil. Int J Hydrogen Energy 2012;37:6447-72.

714 [78] Yang G, Yu H, Peng F, Wang H, Yang J, Xie D Thermodynamic analysis of
715 hydrogen generation via oxidative steam reforming of glycerol. Renewable Energy
716 2011;36:2120-7.

717 [79] Chen J, Tamura M, Nakagawa Y, Okumura K, Tomishige K Promoting effect of
718 trace pd on hydrotalcite-derived Ni/Mg/Al catalyst in oxidative steam reforming of
719 biomass tar. Appl Catal B Environ 2015;179:412-21. doi:10.1016/j.apcatb.2015.05.042.

720 [80] Erkiaga A, Lopez G, Amutio M, Bilbao J, Olazar M Influence of operating
721 conditions on the steam gasification of biomass in a conical spouted bed reactor. Chem
722 Eng J 2014;237:259-67.

723 [81] Luo S, Xiao B, Hu Z, Liu S, Guo X, He M Hydrogen-rich gas from catalytic steam
724 gasification of biomass in a fixed bed reactor: Influence of temperature and- steam on
725 gasification performance. Int J Hydrogen Energy 2009;34:2191-4.

726 [82] Umeki K, Yamamoto K, Namioka T, Yoshikawa K High temperature steam-only
727 gasification of woody biomass. Appl Energy 2010;87:791-8.

728 [83] Miyazawa T, Kimura T, Nishikawa J, Kado S, Kunimori K, Tomishige K Catalytic
729 performance of supported Ni catalysts in partial oxidation and steam reforming of tar
730 derived from the pyrolysis of wood biomass. Catal Today 2006;115:254-62.

731 [84] Yao D, Wu C, Yang H, et al. Hydrogen production from catalytic reforming of the
732 aqueous fraction of pyrolysis bio-oil with modified Ni-Al catalysts. Int J Hydrogen
733 Energy 2014;39:14642-52.

734 [85] Iovane P, Donatelli A, Molino A Influence of feeding ratio on steam gasification
735 ofpalm shells in a rotary kiln pilot plant. Experimental and numerical investigations.
736 Biomass Bioenergy 2013;56:423-31.

737 [86] Gil J, Corella J, Aznar MP, Caballero MA Biomass gasification in atmospheric and
738 bubbling fluidized bed: Effect of the type of gasifying agent on the product distribution.
739 Biomass and Bioenergy 1999;17:389-403.

740